Received: 6 March 2020 | Revised: 19 August 2020 | Accepted: 26 August 2020

DOI: 10.1002/bit.27547

ARTICLE

BIOTECHNOLOGY AND BIOENGINEERING WILEY

Strain engineering for high-level 5-aminolevulinic acid production in *Escherichia coli*

Dragan Miscevic[1] | Ju-Yi Mao[2] | Teshager Kefale[1,3] | Daryoush Abedi[1,4] | Murray Moo-Young[1] | C. Perry Chou[1]

[1]Department of Chemical Engineering, University of Waterloo, Waterloo, Ontario, Canada

[2]Department of Bioscience and Biotechnology, National Taiwan Ocean University, Keelung, Canada

[3]Department of Biology, University of Waterloo, Waterloo, Ontario, Canada

[4]Department of Drug & Food Control, Tehran University of Medical Sciences, Tehran, Iran

Correspondence

C. Perry Chou, Department of Chemical Engineering, University of Waterloo, 200 University Avenue West, Waterloo, Ontario, Canada N2L 3G1.
Email: cpchou@uwaterloo.ca

Funding information

Natural Sciences and Engineering Research Council of Canada, Grant/Award Numbers: Canada Research Chair (CRC) grant 950-211471, Strategic Partnership grant 430106-12

Abstract

Herein, we report the development of a microbial bioprocess for high-level production of 5-aminolevulinic acid (5-ALA), a valuable non-proteinogenic amino acid with multiple applications in medical, agricultural, and food industries, using *Escherichia coli* as a cell factory. We first implemented the Shemin (i.e., C4) pathway for heterologous 5-ALA biosynthesis in *E. coli*. To reduce, but not to abolish, the carbon flux toward essential tetrapyrrole/porphyrin biosynthesis, we applied clustered regularly interspersed short palindromic repeats interference (CRISPRi) to repress *hemB* expression, leading to extracellular 5-ALA accumulation. We then applied metabolic engineering strategies to direct more dissimilated carbon flux toward the key precursor o f succinyl-CoA for enhanced 5-ALA biosynthesis. Using these engineered *E. coli* strains for bioreactor cultivation, we successfully demonstrated high-level 5-ALA biosynthesis from glycerol (~30 g L^{-1}) under both microaerobic and aerobic conditions, achieving up to 5.95 g L^{-1} (36.9% of the theoretical maximum yield) and 6.93 g L^{-1} (50.9% of the theoretical maximum yield) 5-ALA, respectively. This study represents one of the most effective bio-based production of 5-ALA from a structurally unrelated carbon to date, highlighting the importance of integrated strain engineering and bioprocessing strategies to enhance bio-based production.

KEYWORDS

5-aminolevulinic acid, *Escherichia coli*, glycerol, glyoxylate shunt, strain engineering, succinyl-CoA, TCA cycle

1 | INTRODUCTION

5-Aminolevulinic acid (5-ALA) is a non-proteinogenic amino acid existing in most living organisms as a metabolic intermediate toward biosynthesis of essential tetrapyrrole/porphyrin pigment compounds, such as heme (Schlicke et al., 2015; Figure 1). Practically, 5-ALA has broad applications in many fields, such as medicine (Inoue, 2017; Juzeniene, Juzenas, Iani, & Moan, 2002), agriculture (Hotta, Tanaka, Takaoka, Takeuchi, & Konnai, 1997), and food preservation (Y. Li, Li, & Wang, 2016). In nature, there are two major metabolic routes for 5-ALA biosynthesis: the C4 (or Shemin) pathway and the C5 pathway. The Shemin pathway, commonly found in mammals, fungi, and purple sulphur bacteria, fuses succinyl-CoA and glycine via a 5-aminolevulinate synthase (ALAS or HemA) to form 5-ALA (Kang et al., 2004). In the C5 pathway, commonly found in most bacteria (including *Escherichia coli*), all archaea and plants, 5-ALA is generated via a three-step reaction which includes the ligation of glutamate and $tRNA^{Glu}$ by glutamyl-tRNA synthase (GluTS) to form L-glutamyl-tRNA, the subsequent reduction by glutamyl-tRNA reductase (GluTR or HemA) to form glutamate-1-semialdehyde (GSA), and the final transamination by glutamate-1-semialdehyde-2,1-aminomutase (GSAM or HemL; Woodard & Dailey, 1995).

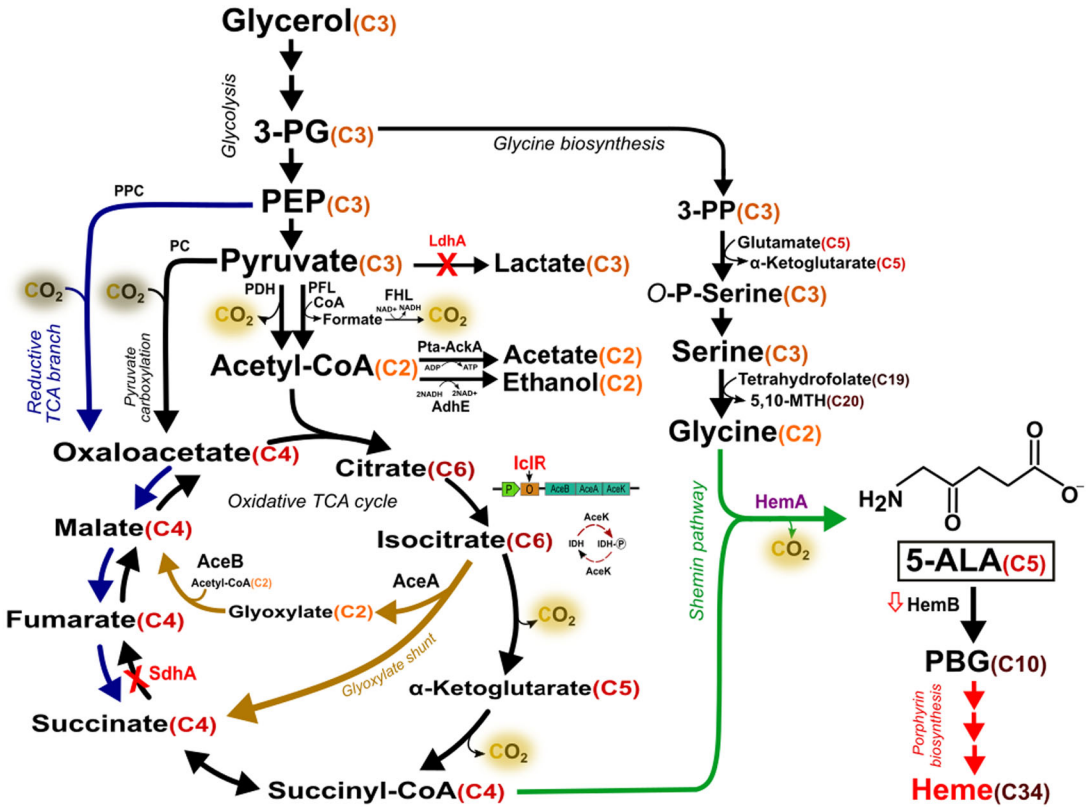

FIGURE 1 Schematic representation of the natural metabolism and the implemented Shemin pathway for 5-ALA and porphyrin biosynthesis in *E. coli* from glycerol. Metabolic pathways outlined: glycolysis, glycine biosynthesis, pyruvate carboxylation, and oxidative TCA cycle (in black); glyoxylate shunt in the TCA cycle (in light brown); reductive branch of TCA cycle (in blue); Shemin pathway (in green); porphyrin biosynthesis (in red). Colored proteins: mutations (in red); overexpression (in purple). The number of carbon atoms for each metabolite is specified in orange. 5,10-MTH, 5,10-methenyltetrahydrofolic acid; 5-ALA, 5-aminolevulinic acid; 3-PG, 3-phosphoglycerate; 3-PP, 3-phosphooxypyruvate; AceA, isocitrate lyase; AceB, malate synthase A; AceK, isocitrate dehydrogenase kinase/phosphatase; AckA, acetate kinase; AdhE, aldehyde-alcohol dehydrogenase; FHL, formate hydrogenlyase; HemA, 5-aminolevulinate synthase; HemB, 5-aminolevulinate dehydratase; IclR, AceBAK operon repressor; IDH, isocitrate dehydrogenase; IDH-P, isocitrate dehydrogenase-phosphate; LdhA, lactate dehydrogenase A; O-P-Serine, O-phospho-l-serine; PBG, porphobilinogen; PC, pyruvate carboxylase; PckA, phosphoenolpyruvate carboxykinase; PDH, pyruvate dehydrogenase; PEP, phosphoenolpyruvate; PFL, pyruvate formate-lyase; PK, pyruvate kinase; PPC, phosphoenolpyruvate carboxylase; Pta, phosphotransacetylase; SdhA, succinate dehydrogenase complex (subunit A) [Color figure can be viewed at wileyonlinelibrary.com]

While 5-ALA can be chemically derived from various precursors, such as levulinic acid (MacDonald, 1974), tetrahydrofurfurylamine (Kawakami, Ebata, & Matsushita, 1991), 5-bromo esters (Ha, Lee, Ha, & Park, 1994), and *N*-furfurylphthalimide (Takeya, Ueki, Miyanari, Shimizu, & Kojima, 1996), these synthetic approaches are deemed uneconomical and the production processes are often complicated for implementation with low yields (Kang et al., 2017). As a result, bio-based production of 5-ALA using either multi-enzyme systems (Meng et al., 2016) or various cell factories has been explored (Sasaki, Watanabe, Tanaka, & Tanaka, 2002), in particular photosynthetic microorganisms, such as *Rhodobacter sphaeroides*, *Rhodopseudomonas palustris*, and *Chlorella* sp. (Sasaki, Watanabe, Tanaka, Hotta, & Nagai, 1995), *Streptomyces coelicolor* (Tran, Pham, & Kim, 2019), *Corynebacterium glutamicum* (Zhang & Ye 2018), as well as genetically tractable *E. coli* (Ding, Weng, Du, Chen, & Kang, 2017; Zhang, Kang, Chen, & Du, 2015; Zhang, Weng, Zhou, Du, & Kang, 2019).

5-ALA serves as precursor for essential porphyrin compounds and is among the most conserved metabolites across all biological kingdoms (Petříčková et al., 2015; Yu, Jin, Liu, Wang, & Qi, 2015). In virtually all biological systems, porphyrins, such as heme, serve as a prosthetic group in many essential proteins (e.g., cytochromes and heme-containing globins; Asakura & Yonetani, 1969; Y. Li, Hsieh, Henion, & Ganem, 1993), and also operate as regulatory molecules in numerous cellular roles/processes (e.g., transcription, translation, protein stability, and differentiation; Padmanaban, Venkateswar, & Rangarajan, 1989; Ponka, 1999). Given the imperative physiological role of porphyrin compounds, attempting to accumulate 5-ALA by inactivation of the immediate post-5-ALA conversion catalyzed by 5-aminolevulinate dehydratase (HemB, encoded by *hemB*) would abolish porphyrin biosynthesis (Figure 1) and, therefore, be detrimental to the cells. Previous attempts at *hemB* repression in *E. coli* through direct engineering of the *hemB* open reading frame (ORF; Kang, Wang, Gu, Wang, & Qi, 2011) and start codon (Ding et al., 2017) were not particularly effective in accumulating 5-ALA. On the other hand, at the expense of impaired cell growth, effective downregulation of *hemB* expression for 5-ALA production in *E. coli*

was made by direct promoter substitution strategies, that is, implementing low-strength and stationary-phase constitutive promoters (Zhang et al., 2019). Recently, Clustered Regularly Interspersed Short Palindromic Repeats interference (CRISPRi) was applied to effectively repress *hemB* expression in *E. coli* for 5-ALA production (Su et al., 2019). However, the study adopted the native C5 pathway which could be metabolically and energetically limited as this route requires the expression of multiple tightly regulated enzymes (Wang, Elliott, & Elliott, 1999), utilization of ATP/NADPH as limiting cofactors (J. M. Li, Brathwaite, Cosloy, & Russell, 1989), and formation of unstable GSA intermediates (O'Brian, 2009).

Considering the above technical aspects/limitations, we chose to implement the Shemin pathway into *E. coli* for heterologous 5-ALA biosynthesis with metabolic direction of the dissimilated carbon flux toward the oxygen-sensitive formation of succinyl-CoA in the tricarboxylic acid (TCA) cycle. In *E. coli*, succinate (and, therefore, succinyl-CoA) can be derived via three oxygen-dependent pathways, (i) reductive TCA branch, (ii) oxidative TCA cycle, and (iii) glyoxylate shunt (Figure 1; Cheng, Wang, Zeng, & Zhang, 2013). Under anaerobic conditions, succinate serves as an electron acceptor (instead of oxygen) and accumulates as an end-product of mixed acid fermentation via the reductive TCA branch (Thakker, Martinez, San, & Bennett, 2012). Although the reductive TCA branch can potentially yield high-level succinate, this pathway is generally unfavorable due to the limited availability of reducing equivalents (Skorokhodova, Morzhakova, Gulevich, & Debabov, 2015). Under aerobic conditions, succinate is normally used up as a metabolic intermediate of the oxidative TCA cycle without accumulation, except for the conditions of oxidative stress and/or acetate/fatty-acid consumption under which succinate can be aerobically derived via the operational glyoxylate shunt (Thakker et al., 2012). Moreover, without supplementation of structurally related carbons, glycerol can be used as the major carbon source for cultivation of engineered *E. coli* strains due to its low cost (Ciriminna, Pina, Rossi, & Pagliaro, 2014) and highly reduced nature, generating approximately twice the number of reducing equivalents upon its degradation compared to traditional fermentable sugars (Murarka, Dharmadi, Yazdani, & Gonzalez, 2008; Yazdani & Gonzalez, 2007).

Aside from mutation of competing metabolic pathway genes, repression of endogenous genes has often been used as an alternative method for balancing metabolic fluxes inside of the cell (Kim, Seong, Han, Lee, & Lee, 2017). Advantages of gene repression include the ability to modulate gene expression with minimum or even no modifications to the genome and to fine-tune target gene expression to balance cell growth and biosynthesis of target metabolites (Wu, Yu, Du, Zhou, & Chen, 2014). Development of CRISPRi technology has enabled a more rigorously controlled gene expression at the transcriptional level through interfering with initiation or elongation of transcription by targeting RNA polymerase. While CRISPRi implementation is rather easy to perform, only a handful of studies have applied it to balance the metabolic network for maximizing titer/yield levels (Cress et al., 2017; Kim et al., 2016; S. Li, Jendresen, et al., 2016; Woolston, Emerson, Currie, & Stephanopoulos, 2018).

In this study, we explored strain engineering strategies for high-level 5-ALA production in *E. coli* using the Shemin pathway. Unlike the previous study which targeted the coding sequence and ribosome bind site region of *hemB* (Su et al., 2019), we applied CRISPRi by targeting various sequences in the promoter and ORF regions for reduced expression. As a result of our *hemB*-repression strategy, our engineered *E. coli* strain increased 5-ALA accumulation without imposing physiological impacts to the producing cells. Using various engineered *E. coli* strains for bioreactor cultivation, we demonstrated high-level 5-ALA biosynthesis under both microaerobic and aerobic conditions with glycerol as a major carbon source.

2 | MATERIALS AND METHODS

2.1 | Bacterial strains and plasmids

Bacterial strains and plasmids used in this study are listed Table 1, while oligonucleotide sequences are presented in Table S1. Genomic DNA from bacterial cells was isolated using the Blood & Tissue DNA Isolation Kit (Qiagen). Standard recombinant DNA technologies were applied for molecular cloning (Miller, 1992). *Taq* DNA polymerase was obtained from New England Biolabs (Ipswich). All synthesized oligonucleotides were obtained from Integrated DNA Technologies (Coralville). DNA sequencing was conducted by the Centre for Applied Genomics at the Hospital for Sick Children (Toronto, Canada). *E. coli* BW25113 was the parental strain for derivation of all engineered strains in this study and *E. coli* DH5α was used as a host for molecular cloning. Note that the *ldhA* gene (encoding lactate dehydrogenase) was previously inactivated in BW25113, generating BWΔ*ldhA* (Srirangan et al., 2014), a strain with higher metabolic potential as it limits side production of lactate.

For genetic implementation of the Shemin pathway in *E. coli*, the *hemA* gene was first amplified by polymerase chain reaction (PCR) using the primer set g-hemA and the genomic DNA of wild-type *Rhodobacter sphaeroides* DSM 158 as the template. The amplified *hemA* gene was Gibson-assembled with the PCR-linearized pK184 using the primer set g-pK-hemA to generate pK-hemA. The expression of the cloned *hemA* gene in the pK184 vector was under the control of the P_{lac} promoter.

Knockouts of the genes, including *sdhA* [encoding succinate dehydrogenase (SDH) complex flavoprotein subunit A, SdhA] and *iclR* (encoding transcriptional AceBAK operon repressor, IclR), were introduced into BWΔ*ldhA* by P1 phage transduction (Miller, 1992) using the appropriate Keio Collection strains (The Coli Genetic Stock Center, Yale University) as donors (Baba et al., 2006). To eliminate the co-transduced FRT-Kn^R-FRT cassette, the transductants were transformed with pCP20 (Cherepanov & Wackernagel, 1995), a temperature-sensitive plasmid expressing a flippase (Flp) recombinase. Upon Flp-mediated excision of the Kn^R cassette, a single Flp recognition site (FRT "scar site") was generated. Plasmid pCP20 was then cured by growing cells at 42°C. The genotypes of derived knockout strains were confirmed by colony PCR using the appropriate verification primer sets listed in Table S1.

TABLE 1 *E. coli* strains and plasmids used in this study

Name	Description or relevant genotype	Source
***E. coli* host strains**		
DH5α	F−, *endA1*, *glnV44*, *thi-1*, *recA1*, *relA1*, *gyrA96*, *deoR*, *nupG φ80d lacZΔacZd ladlacZYA − argF) U169*, *hsdR17(rK-mK +)*, *λ-*	Lab stock
BW25113	F-, *Δ(araD-araB)567*, *ΔlacZ4787(::rrnB-3)*, *λ-*, *rph-1*, *Δ(rhaD-rhaB)568*, *hsdR514*	Datsenko and Wanner (2000)
BWΔ*ldhA*	BW25113 *ldhA* null mutant	Srirangan et al. (2014)
DMH	BWΔ*ldhA*/pK-hemA	This study
DMHΔ*sdhA*	*sdhA* null mutant of DMH	This study
DMHΔ*sdhA*Δ*iclR*	*sdhA* and *iclR* mutants of DMH	This study
DMH-CT	DMH/pK-hemA/pgRNA-bacteria/pdcas9-bacteria	This study
DMH-L1	DMH/pK-hemA/pgRNA-L1/pdcas9-bacteria	This study
DMH-L2	DMH/pK-hemA/pgRNA-L2/pdcas9-bacteria	This study
DMH-L3	DMH/pK-hemA/pgRNA-L3/pdcas9-bacteria	This study
DMH-L4	DMH/pK-hemA/pgRNA-L4/pdcas9-bacteria	This study
DMH-L4Δ*sdhA*	*sdhA* null mutant of DMH-L4	This study
DMH-L4Δ*iclR*	*iclR* null mutant of DMH-L4	This study
DMH-L4Δ*sdhA*Δ*iclR*	*sdhA* and *iclR* null mutants of DMH-L4	This study
Plasmids		
pCP20	Flp+, λ cI857+, λ pR Rep(pSC101 ori)ts, ApR, CmR	Cherepanov and Wackernagel (1995)
pK184	p15A ori, KmR, P*lac*::*lacZ′*	Jobling and Holmes (1990)
pdcas9-bacteria	p15A ori, P_{Tet}-dCas9	Qi et al. (2013)
pgRNA-bacteria	ColE1 origin, P_{J23119}-gRNA	Qi et al. (2013)
pgRNA-L1	Derived from pgRNA-bacteria, P_{spel}::*hemB*-gRNA-L1	This study
pgRNA-L2	Derived from pgRNA-bacteria, P_{spel}::*hemB*-gRNA-L2	This study
pgRNA-L3	Derived from pgRNA-bacteria, P_{spel}::*hemB*-gRNA-L3	This study
pgRNA-L4	Derived from pgRNA-bacteria, P_{spel}::*hemB*-gRNA-L4	This study
pK-hemA	Derived from pTrc99a, P_{trc}::*phaAB*	This study

The expression of *hemB* was repressed by CRISPRi using various derived plasmids from pdcas9-bacteria (Addgene plasmid #44249) and pgRNA-bacteria (Addgene plasmid #44251). All sgRNAs (*hemB*-targetting sequences) were designed using the online tool ChopChop (Labun, Montague, Gagnon, Thyme, & Valen, 2016) based on predicted expression efficiencies ranging from approximately 35% to 55%. All synthesized oligonucleotide pairs have 60 nucleotides (nt), which includes 20 nt *hemB*-targeting sequence, 20 nt upstream and 20 nt downstream sequences of pgRNA-bacteria vector (Figure 2). They were ordered from Integrated DNA Technologies (Coralville) and annealed as described previously (Pengpumkiat, Koesdjojo, Rowley, Mockler, & Remcho, 2016), generating four double-stranded DNA fragments of *hemB*-gRNA-L1, *hemB*-gRNA-L2, *hemB*-gRNA-L3, and *hemB*-gRNA-L4 (Table S1). All these four DNA fragments were individually Gibson-assembled with the PCR-linearized pgRNA-bacteria using the primer set g-pgRNA to generate pgRNA-L1, pgRNA-L2, pgRNA-L3, and pgRNA-L4, respectively (Table 1). The four *hemB*-repressed strains, that is, DMH-L1, DMH-L2, DMH-L3, and DMH-L4, were developed by creating a triple-plasmid system (Figure 2) containing pK-hemA, pdcas9-bacteria, and the gRNA-containing plasmid (i.e., pgRNA-L1, pgRNA-L2, pgRNA-L3, or pgRNA-L4). For the control strain DMH-CT, the original pgRNA-bacteria plasmid without any *hemB*-targeting sequence was used as the third plasmid.

2.2 | Media and bacterial cell cultivation

All medium components were obtained from Sigma-Aldrich Co. (St Louis) except yeast extract and tryptone which were obtained from BD Diagnostic Systems (Franklin Lakes). *E. coli* strains, stored as glycerol stocks at −80°C, were streaked on lysogeny broth (LB;

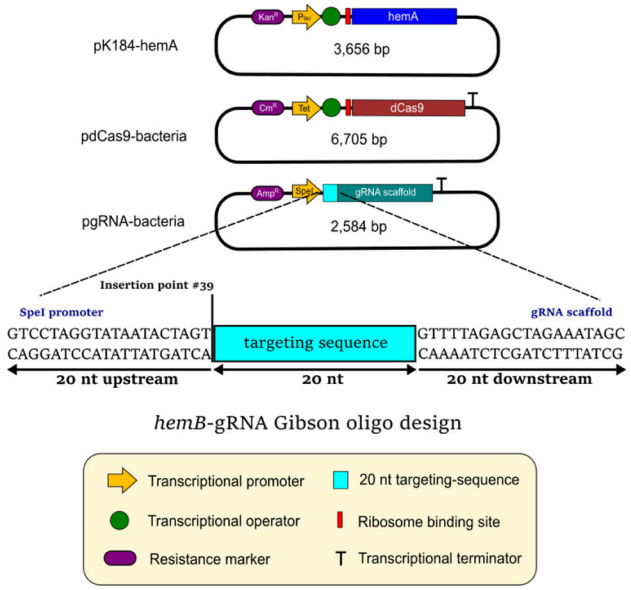

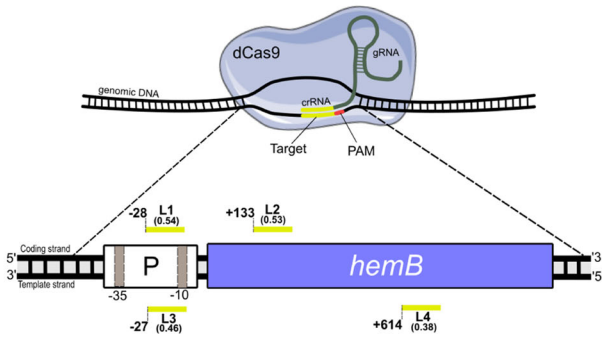

gRNA	20 nt targeting-sequence
hemB-gRNA-L1	CCCTCGATTCCACAAACATC
hemB-gRNA-L2	AAAGCCGTTGAAGCCATGCC
hemB-gRNA-L3	GCCTGATGTTTGTGGAATCG
hemB-gRNA-L4	ATGCGCTTCCGGCAGCTTCA

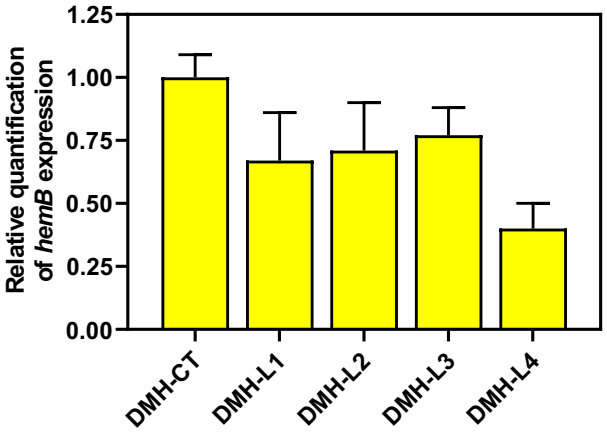

FIGURE 2 Design strategy for CRISPRi-mediated *hemB* repression. The three plasmids with their major genetic features, such as promoters, selection markers, key genes, are shown. The design of *hemB*-targeting sequences and their associated interacting spots in the *hemB* gene (i.e., L1, L2, L3, and L4) and the predicted repression efficiencies (numbers in parenthesis) are shown. The resulting *hemB*-repressed strains, that is, DMH-CT (control), DMH-L1, DMH-L2, DMH-L3, and DMH-L4 were characterized for quantification of the relative *hemB* expression using qRT-PCR. All qRT-PCR values are reported as means ± *SD* ($n = 2$). CRISPRi, clustered regularly interspersed short palindromic repeats interference; qRT-PCR, real-time quantitative reverse transcription polymerase chain reaction [Color figure can be viewed at wileyonlinelibrary.com]

10 g L^{-1} tryptone, 5 g L^{-1} yeast extract, and 5 g L^{-1} NaCl) agar plates and incubated at 37°C for 14–16 h.

For shake-flask cultivations, single colonies were picked from LB plates to inoculate 30 ml LB medium in 125 ml conical flasks. The cultures were shaken at 37°C and 280 rpm in a rotary shaker (New Brunswick Scientific) and used as seed cultures to inoculate 220 ml LB media at 1% (vol/vol) in 1 L conical flasks. This second seed culture was shaken at 37°C and 280 rpm until a cell density of 0.80 OD_{600} was reached. Cells were then harvested by centrifugation at 9000*g* and 20°C for 10 min and resuspended in 30 ml modified M9 production media. The suspended culture was transferred into a 125 ml screwed cap plastic production flasks and incubated at 37°C at 280 rpm in a rotary shaker. Unless otherwise specified, the modified M9 production medium contained 20 g L^{-1} glycerol, 5 g L^{-1} yeast extract, 10 mM $NaHCO_3$, 1 mM $MgCl_2$, 200 ml L^{-1} of M9 salts mix (33.9 g L^{-1} Na_2HPO_4, 15 g L^{-1} KH_2PO_4, 5 g L^{-1} NH_4Cl, 2.5 g L^{-1} NaCl), 1 ml L^{-1} dilution of Trace Metal Mix A5 (2.86 g L^{-1} H_3BO_3, 1.81 g L^{-1} $MnCl_2{\cdot}4H_2O$, 0.222 g L^{-1} $ZnSO_4{\cdot}7H_2O$, 0.39 g L^{-1} $Na_2MoO_4{\cdot}2H_2O$, 79 μg L^{-1} $CuSO_4{\cdot}5H_2O$, 49.4 μg L^{-1} $Co(NO_3)_2{\cdot}6H_2O$), and was supplemented with 0.1 mM isopropyl β-D-1-thiogalactopyranoside (IPTG). All shake-flask cultivation experiments were performed in triplicate.

For bioreactor cultivations, single colonies were picked from LB plates to inoculate 30 ml super broth (SB) medium (32 g L^{-1} tryptone, 20 g L^{-1} yeast extract, and 5 g L^{-1} NaCl) in 125 ml conical flasks. The overnight cultures were shaken at 37°C and 280 rpm in a rotary shaker (New Brunswick Scientific) and used as seed cultures to inoculate 220 ml SB media at 1% (vol/vol) in 1 L conical flasks. This second seed culture was shaken at 37°C and 280 rpm for 14–16 h. Cells were then harvested by centrifugation at 9000*g* and 20°C for 10 min and resuspended in 50 ml fresh LB media. The suspended culture was used to inoculate a 1 L stirred tank bioreactor (containing two Rushton radial flow disks as impellers; CelliGen 115, Eppendorf AG) at 37°C and 430 rpm. The semi-defined production medium in the batch bioreactor contained 30 g L^{-1} glycerol, 0.23 g L^{-1} K_2HPO_4, 0.51 g L^{-1} NH_4Cl, 49.8 mg L^{-1} $MgCl_2$, 48.1 mg L^{-1} K_2SO_4, 1.52 mg L^{-1} $FeSO_4$, 0.055 mg L^{-1} $CaCl_2$, 2.93 g L^{-1} NaCl, 0.72 g L^{-1} tricine, 10 g L^{-1} yeast extract, 10 mM $NaHCO_3$, and 1 ml L^{-1} trace elements (2.86 g L^{-1} H_3BO_3, 1.81 g L^{-1} $MnCl_2{\cdot}4H_2O$, 0.222 g L^{-1} $ZnSO_4{\cdot}7H_2O$, 0.39 g L^{-1} $Na_2MoO_4{\cdot}2H_2O$, 79 μg L^{-1} $CuSO_4{\cdot}5H_2O$, 49.4 μg L^{-1} $Co(NO_3)_2{\cdot}6H_2O$; Neidhardt, Bloch, & Smith, 1974), and was supplemented with 0.1 mM isopropyl IPTG. Microaerobic and semiaerobic conditions were maintained by purging air into the headspace and bulk culture, respectively, at

0.1 vvm, designated as aeration level I (AL-I) and II (AL-II). Aerobic conditions were maintained by purging air into the bulk culture at 1 vvm (AL-III). The pH of the production culture was maintained at 7.0 ± 0.1 with 30% (vol/vol) NH_4OH and 15% (vol/vol) H_3PO_4.

2.3 | Analysis

Culture samples were appropriately diluted with 0.15 M saline solution for measuring cell density in OD_{600} using a spectrophotometer (DU520, Beckman Coulter). Cell-free medium was prepared by centrifugation of the culture sample at 9000*g* for 5 min, followed by filter sterilization using a 0.2 μM syringe filter. Extracellular metabolites and glycerol were quantified using high-performance liquid chromatography (HPLC; LC-10AT; Shimadzu) with a refractive index detector (RID; RID-10A; Shimadzu) and a chromatographic column (Aminex HPX-87H; Bio-Rad Laboratories). The HPLC column temperature was maintained at 35°C and the mobile phase was 5 mM H_2SO_4 (pH 2) running at 0.6 ml min^{-1}. The RID signal was acquired and processed by a data processing unit (Clarity Lite, DataApex, Prague, Czech Republic).

The 5-ALA titer in the cell-free medium was measured using a modified Ehrlich's reagent (Mauzerall & Granick, 1956). The percentage yield of 5-ALA was defined as the mole (or mass) ratio of the produced 5-ALA to the theoretically maximal 5-ALA produced based on the consumed glycerol with a molar ratio of one-to-three (i.e., one mole 5-ALA produced per three moles glycerol consumed). Note that one-mole succinyl-CoA (derived from two-mole glycerol) and one-mole glycine (derived from one-mole glycerol) are required to generate one-mole 5-ALA. The bulk level of secreted porphyrin compounds in the cell-free medium was estimated using a spectrophotometer at two specific wavelengths, that is, 405 nm (measuring Soret band) and 495 nm (measuring collective Q-bands).

2.4 | Real-time quantitative reverse transcription PCR (qRT-PCR)

Cells used for RNA extraction were cultivated in 30 ml liquid LB medium at 37°C and harvested in the exponential growth phase. Total RNA of *E. coli* was extracted using the High Pure RNA Isolation Kit (Roche Diagnostics) according to manufacturer's instructions. Complementary DNAs (cDNAs) were synthesized using the High-Capacity cDNA Reverse Transcription Kit (Thermo Fisher Scientific). Sequence-specific primers were used for reverse transcription of *hemB* mRNA (i.e., q-hemB) and internal control *rrsA* (encoding ribosomal RNA 16S) mRNA (i.e., q-rrsA; Table S1), at a final concentration of 1 μM. One hundred nanograms of the total RNA was used in a 20 μL reaction mixture. Real-time qRT-PCR was carried out using the Power SYBR® Green PCR Master Mix (Thermo Fisher Scientific) in an Applied Biosystems StepOnePlus™ System as per the manufacturer's instructions. All experiments were performed in duplicate.

2.5 | Statistical analysis

All experiments in this study were conducted in either triplicate (for shake-flask cultivations) or duplicate (for bioreactor cultivations). In addition, all data comparisons were statistically analyzed with an unpaired two-tail Student's *t*-test with 95% confidence intervals being used to determine statistical significance (Table S3). Hence, $p < .05$ was used as a standard criterion of statistical significance when comparing the means of 5-ALA titers.

3 | RESULTS

3.1 | Repression of hemB expression for extracellular 5-ALA accumulation

We first implemented the Shemin pathway by episomal expression of *hemA* from *R. sphaeroides* in BWΔ*ldhA*, deriving DMH. The effects of the implemented Shemin pathway were observed by comparing the two cultures of BWΔ*ldhA* and DMH in screw-cap shake-flasks containing 20 g L^{-1} glycerol as the carbon source. Note that all percentage yields of 5-ALA reported in this study were calculated based on the ratio of the produced 5-ALA to the theoretical maximum based on consumed glycerol. While BWΔ*ldhA* generated no detectable levels of 5-ALA or porphyrin, DMH produced 0.44 g L^{-1} 5-ALA (5.22% yield) with considerable porphyrin biosynthesis (Figure 3), suggesting that the Shemin pathway was active in DMH. In particular, the dark red color of the DMH culture (Figure 3) suggests that a substantial amount of glycerol was converted to porphyrin pigments with limited 5-ALA accumulation.

To prevent the above intracellular drainage of 5-ALA, we explored gene knockout of *hemB*, but failed to derive the corresponding mutant strain (data not shown), confirming that *hemB* is an essential gene. We then aimed to reduce the carbon flux toward porphyrin biosynthesis in DMH by repressing the expression of *hemB* (Figure 1), leading to a limited conversion of two 5-ALA molecules into porphobiliongen (PBG) and extracellular 5-ALA accumulation. We applied CRISPRi by designing four *hemB*-targeting gRNAs with different relative expression efficiencies (as predicted by the Chop-Chop online tool), generating four corresponding strains of DMH-L1, DMH-L2, DMH-L3, and DMH-L4 (Figure 3). Note that DMH-CT is the control strain without a *hemB*-specific gRNA for CRISPRi. While cell growth and glycerol consumption were minimally affected for all the triple-plasmid systems, suggesting that these strains had sufficient biosynthesis of essential porphyrins, all *hemB*-repressed strains showed increased extracellular 5-ALA accumulation compared to DMH-CT upon shake-flask cultivation. In particular, DMH-L1 and DMH-L4 had both titers and yields up to 4-5 fold higher than the control strain DMH-CT (5-ALA titers: 1.26 and 1.61 vs. 0.34 g L^{-1}; Figure 3). This significant increase in 5-ALA accumulation in DMH-L1 and DMH-L4 occurred simultaneously with considerably reduced levels of the relative *hemB* expression at 67% and 40%, respectively (Figure 2). Additional supporting evidence for the repressed *hemB*

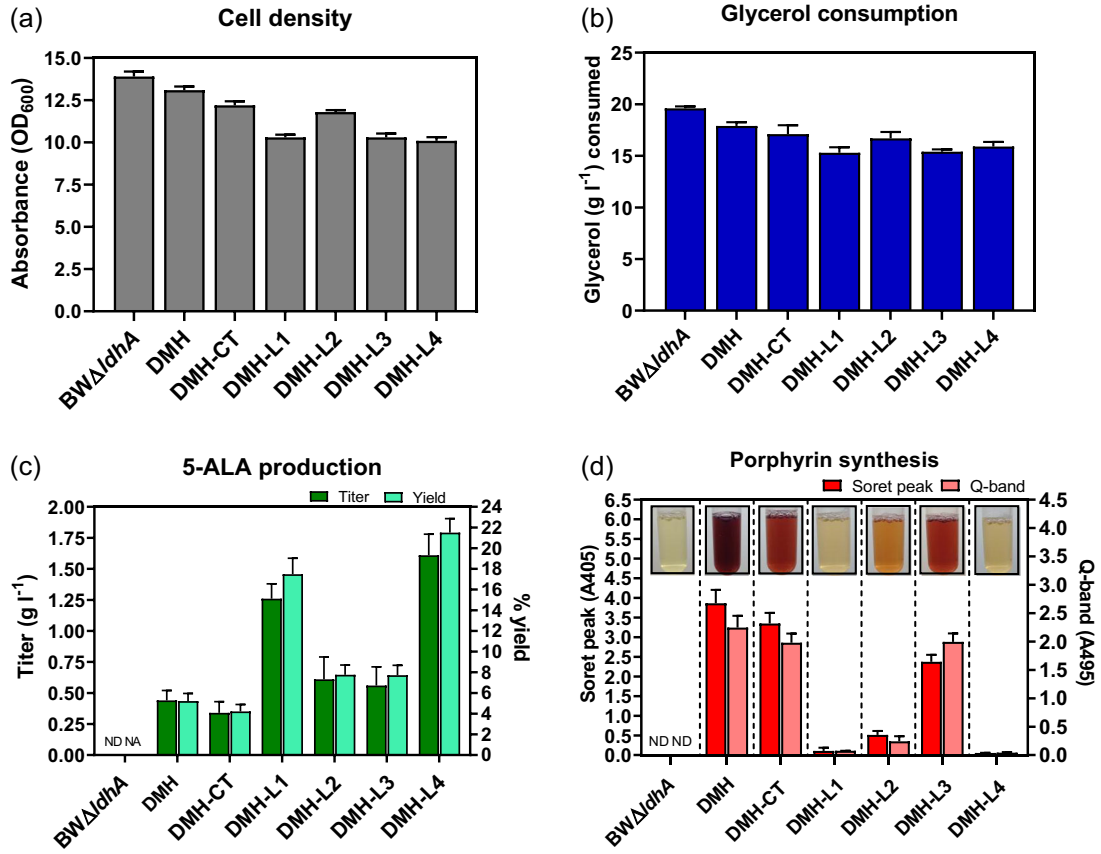

FIGURE 3 Shake-flask cultivation of *hemB*-repressed strains for 5-aminolevulinic acid (5-ALA) accumulation. Strains compared include BWΔ*ldhA*, DMH, DMH-CT, DMH-L1, DMH-L2, DMH-L3, and DMH-L4. Results of the 48 h shake-flask cultivation in (a) cell density (OD_{600}), (b) glycerol consumption, (c) 5-ALA titer and percentage yield, and (d) porphyrin biosynthesis (represented by the absorbance readings of the Soret peak [A405] and Q-band [A495] with the images of cell-free media) are shown. All values are reported as means ± *SD* (*n* = 3) [Color figure can be viewed at wileyonlinelibrary.com]

expression was reflected by the decrease in porphyrin biosynthesis in all four *hemB*-repressed strains as the degrees of pigmentation and the corresponding absorbances (in 405 and 495 nm) of the cell-free media were considerably lower than that of the control strain DMH-CT (Figure 3). Given the lowest relative *hemB* expression and the most superior extracellular 5-ALA accumulation in DMH-L4 among all *hemB*-repressed strains, we used this strain for all subsequent experiments.

3.2 | Effects of oxygenic condition on 5-ALA biosynthesis

5-ALA biosynthesis via the Shemin pathway requires succinyl-CoA as one of the two key precursors. Several metabolic pathways are involved in succinyl-CoA formation in *E. coli*, that is, reductive TCA branch, oxidative TCA cycle, and glyoxylate shunt (Figure 1). These metabolic pathways, along with cell growth and acetogenesis, can be sensitive to the oxygenic condition, which critically directs the dissimilated carbon flux toward succinyl-CoA for 5-ALA biosynthesis. To investigate such oxygenic effects, batch cultivation of the control strain DMH in a bioreactor containing 30 g L^{-1} glycerol (and 10 g L^{-1} yeast extract) was subject to three different levels of aeration, that is, AL-I (microaerobic), AL-II (semiaerobic), and AL-III (aerobic; Figure 4). While cell growth and glycerol consumption were favored by oxygen exposure, 5-ALA biosynthesis was more effective under lower aeration levels, that is, 0.53 g L^{-1} (3.40% yield) under AL-I, 0.39 g L^{-1} (2.44% yield) under AL-II, and 0.31 g L^{-1} (2.08% yield) under AL-III, presumably because more carbon was directed toward the succinyl-CoA node under microaerobic conditions. In addition, the reduced 5-ALA biosynthesis under aerobic conditions occurred with less porphyrin formation, reflected by a notably less pigmentation of the culture medium (complete time-course data is presented in Table S2). Note that, in addition to low levels of 5-ALA biosynthesis in DMH under all investigated culture conditions, acetate was the major side metabolite with high yields up to 75.9%, implying considerable spillover at the acetyl-CoA node. The results suggest that 5-ALA biosynthesis in DMH was rather favored by lower oxygenic levels and potentially limited by acetogenesis. Note that glycerol utilization and cell growth were severely inhibited when DMH was cultivated under a strict anaerobic condition (data not shown).

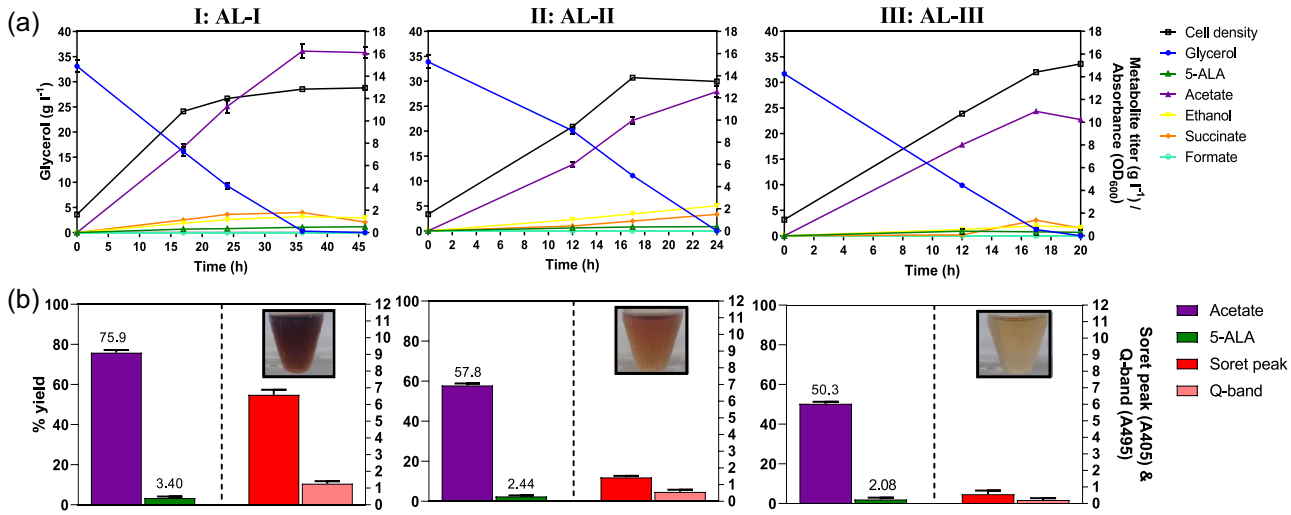

FIGURE 4 Bioreactor cultivation of DMH for 5-aminolevulinic acid (5-ALA) biosynthesis under different oxygenic conditions. (a) Time profiles of cell density (OD_{600}), glycerol consumption and metabolite production profiles. (b) Acetate/5-ALA percentage yields, and porphyrin biosynthesis (represented by the absorbance readings of the Soret peak [A405] and Q-band [A495] with the images of cell-free media). The percentage yields of acetate/5-ALA and absorbance readings of porphyrin compounds are calculated/measured based on the consumed glycerol at the end of cultivation. (I) AL-I: microaerobic, (II) AL-II: semi-aerobic, and (III) AL-III: aerobic. All values are reported as means ± *SD* ($n = 2$) [Color figure can be viewed at wileyonlinelibrary.com]

3.3 | Metabolic engineering to enhance 5-ALA biosynthesis under microaerobic conditions

As previously demonstrated (Arikawa et al., 1999), disruption of SDH complex can reduce acetate secretion under oxygen limitation. Hence, we derived a single-knockout mutant DMHΔ*sdhA*, in which the oxidative TCA cycle was disrupted (Figure 5-I). In addition to reduced acetogenesis under AL-I, DMHΔ*sdhA* produced 0.94 g L^{-1} 5-ALA (6.61% yield) with enhanced formate, succinate, and ethanol secretion. With an increased carbon flux toward porphyrin biosynthesis, pigmentation of the DMHΔ*sdhA* culture medium was moderately enhanced. On the other hand, while glycerol consumption and cell growth were substantially inhibited upon cultivation of the *hemB*-repressed strain DMH-L4 under AL-I, 5-ALA biosynthesis was significantly improved with much-reduced acetogenesis, achieving 4.73 g L^{-1} 5-ALA with 32.0% yield (Figure 5-II; 5-ALA titers: 0.53 vs. 4.73 g L^{-1}). The improved 5-ALA biosynthesis was also evidenced by a considerable reduction in pigmentation of the culture medium compared to DMH. Notably, compared to DMHΔ*sdhA* or DMH-L4, 5-ALA biosynthesis was further improved upon the cultivation of DMH-L4Δ*sdhA*, in which the *sdhA* mutation and *hemB*-repression was simultaneously introduced, under AL-I, achieving 5.95 g L^{-1} 5-ALA with 36.9% yield (Figure 5-III; 5-ALA titers: 0.94 and 4.73 vs. 5.95 g L^{-1}). These results suggest that the dissimilated carbon flux was directed toward the succinyl-CoA node for 5-ALA biosynthesis primarily via the reductive TCA branch under microaerobic conditions, and such carbon flux direction was rather effective upon simultaneous disruption of the oxidative TCA cycle and *hemB* repression. Aside from DMHΔ*sdhA*, higher levels of formate, succinate, and ethanol were also observed upon cultivation of other two engineered strains, that is, DMH-L4 and DMH-L4Δ*sdhA*, in comparison to DMH under microaerobic conditions for enhanced 5-ALA biosynthesis.

3.4 | Metabolic engineering to enhance 5-ALA biosynthesis under aerobic conditions

We also explored 5-ALA biosynthesis under aerobic conditions, which often facilitate carbon utilization and cell growth. While the DMH-L4 culture under AL-III showed effective glycerol dissimilation and cell growth, biosynthesis of 5-ALA and porphyrins was much lower than that of the DMH-L4 culture under AL-I (Figure 6-I vs. 5-II; 5-ALA titers: 1.97 vs. 4.73 g L^{-1}), suggesting a potential limitation in succinyl-CoA precursor under aerobic conditions. Nevertheless, the enhancing effects of *hemB*-repression on 5-ALA biosynthesis were still observable under aerobic conditions by comparing the two cultures of DMH-L4 and DMH under AL-III (Figure 6-I vs. 4-III; 5-ALA titers: 1.97 vs. 0.31 g L^{-1}). To overcome the limitation in succinyl-CoA under AL-III, we derived another mutant of DMH-L4Δ*iclR* with a deregulated glyoxylate shunt. Compared to the parental strain DMH-L4, DMH-L4Δ*iclR* had a much higher 5-ALA biosynthesis with effective glycerol dissimilation and cell growth under AL-III (Figure 6-III vs. 6-I; 5-ALA titers: 5.32 vs. 1.97 g L^{-1}) suggesting successful direction of the dissimilated carbon flux toward succinyl-CoA for 5-ALA biosynthesis via the glyoxylate shunt under aerobic conditions. For more effective carbon flux direction, we derived another double mutant of DMH-L4Δ*iclR*Δ*sdhA* with a disruptive oxidative TCA cycle such that the directed carbon flux at the succinate node via the glyoxylate shunt could be further

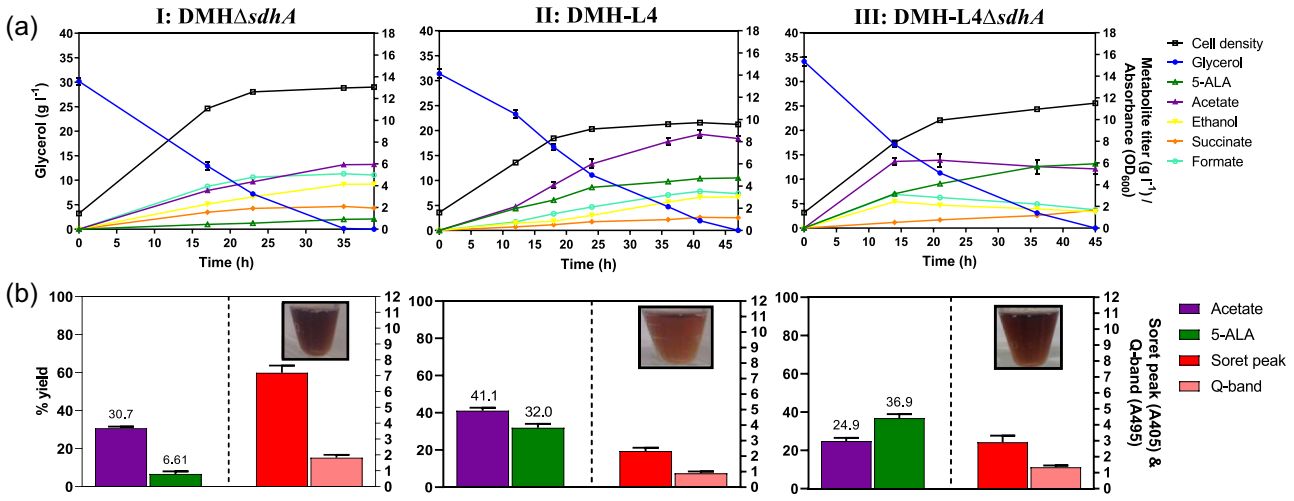

FIGURE 5 Bioreactor cultivation of engineered *Escherichia coli* for 5-aminolevulinic acid (5-ALA) biosynthesis under microaerobic (AL-I) conditions. Strains compared include DMHΔ*sdhA*, DMH-L4, and DMH-L4Δ*sdhA*. (a) Time profiles of cell density (OD_{600}), glycerol consumption, and metabolite production profiles. (b) Acetate/5-ALA percentage yields, and porphyrin biosynthesis (represented by the absorbance readings of the Soret peak [A405] and Q-band [A495] with the images of cell-free media). The percentage yields of acetate/5-ALA and absorbance readings of porphyrin compounds are calculated/measured based on the consumed glycerol at the end of cultivation. (I) DMHΔ*sdhA*, (II) DMH-L4, and (III) DMH-L4Δ*sdhA*. All values are reported as means ± *SD* ($n = 2$) [Color figure can be viewed at wileyonlinelibrary.com]

directed toward succinyl-CoA via the activity of fumarate reductase (FRD) complex. Compared to the parental strain DMH-L4Δ*iclR*, DMH-L4Δ*iclR*Δ*sdhA* had even higher 5-ALA biosynthesis under AL-III (Figure 7-II vs. 6-III), achieving 6.93 g L^{-1} 5-ALA with 50.9% yield (5-ALA titers: 6.93 vs. 5.32 g L^{-1}). On the other hand, the mutation of *sdhA* in DMH-L4Δ*sdhA* appeared to be rather harmful to cell physiology and, therefore, culture performance (Figure 6-II vs. 6-I; 5-ALA titers: 0.51 vs. 1.97 g L^{-1}). Note that the 5-ALA yield for DMH-L4Δ*sdhA*Δ*iclR* was 3.4-fold that for DMH-L4 and 1.3-fold that for DMH-L4Δ*iclR*. Also, note that the enhancing effects of *hemB*-repression on 5-ALA biosynthesis were further confirmed by comparing the two cultures of DMH-L4Δ*iclR*Δ*sdhA* and DMHΔ*iclR*Δ*sdhA* under AL-III (Figure 7-II vs. 7-I; 5-ALA titers: 6.93 vs. 2.51 g L^{-1}). On the other hand, the successful carbon flux direction toward the Shemin pathway via the glyoxylate shunt and partial reductive TCA branch for biosynthesis of both 5-ALA and porphyrin pigments can be also observed by comparing the two cultures of DMHΔ*iclR*Δ*sdhA* and DMH under AL-III (Figure 7-I vs. 4-III; 5-ALA titers: 2.51 vs. 0.31 g L^{-1}).

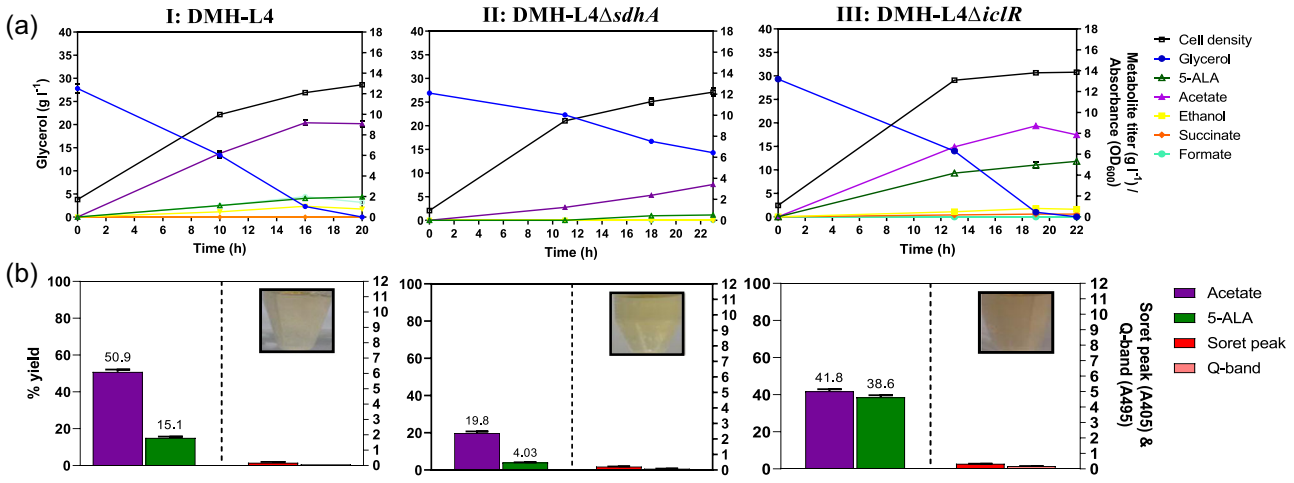

FIGURE 6 Bioreactor cultivation of engineered *Escherichia coli* for 5-aminolevulinic acid (5-ALA) biosynthesis under aerobic (AL-III) conditions. Strains compared include DMH-L4, DMH-L4Δ*sdhA*, and DMH-L4Δ*iclR*. (a) Time profiles of cell density (OD_{600}), glycerol consumption and metabolite production profiles. (b) Acetate/5-ALA percentage yields, and porphyrin biosynthesis (represented by the absorbance readings of the Soret peak [A405] and Q-band [A495] with the images of cell-free media). The percentage yields of acetate/5-ALA and absorbance readings of porphyrin compounds are calculated/measured based on the consumed glycerol at the end of cultivation. (I) DMH-L4, (II) DMH-L4Δ*sdhA*, and (III) DMH-L4Δ*iclR*. All values are reported as means ± *SD* ($n = 2$) [Color figure can be viewed at wileyonlinelibrary.com]

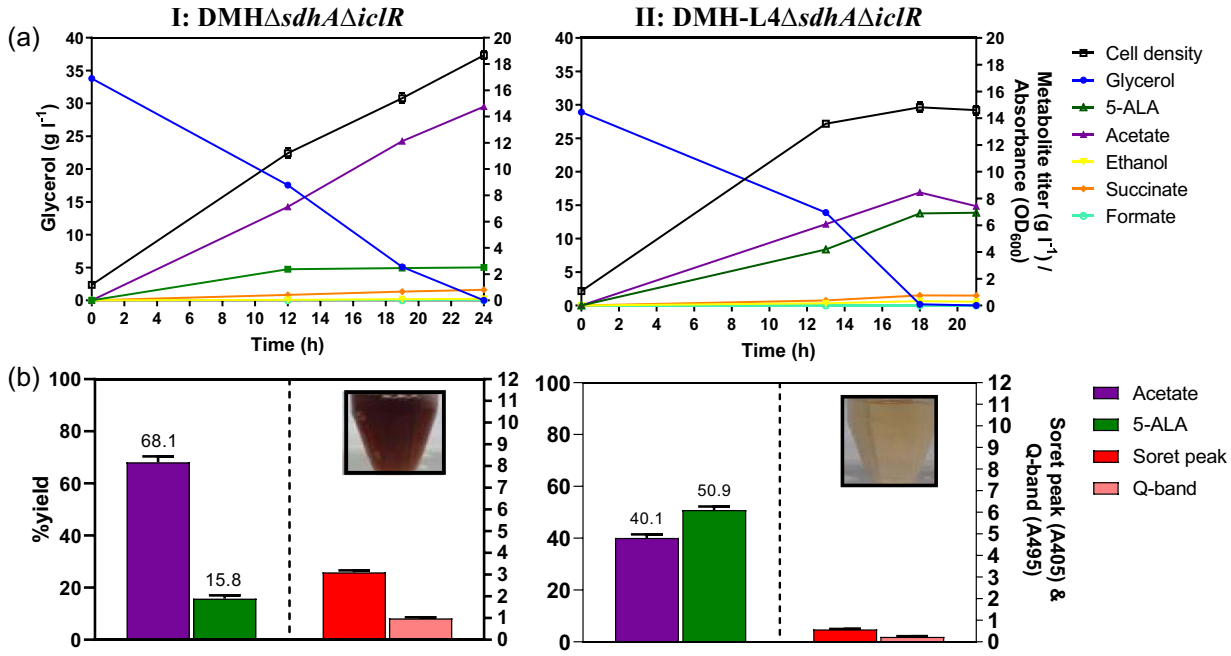

FIGURE 7 Bioreactor cultivation of *Escherichia coli* double mutants for 5-aminolevulinic acid (5-ALA) biosynthesis under aerobic (AL-III) conditions. Strains compared include DMHΔ*sdhA*Δ*iclR* and DMH-L4Δ*sdhA*Δ*iclR*. (a) Time profiles of cell density (OD_{600}), glycerol consumption and metabolite production profiles. (b) Acetate/5-ALA percentage yields, and porphyrin biosynthesis (represented by the absorbance readings of the Soret peak [A405] and Q-band [A495] with the images of cell-free media). The percentage yields of acetate/5-ALA and absorbance readings of porphyrin compounds are calculated/measured based on the consumed glycerol at the end of cultivation. (I) DMHΔ*sdhA*Δ*iclR*, and (II) DMH-L4Δ*sdhA*Δ*iclR*. All values are reported as means ± *SD* ($n = 2$) [Color figure can be viewed at wileyonlinelibrary.com]

These results successfully demonstrated the consolidated strategy based on carbon flux redirection in the TCA cycle toward the Shemin pathway with repressed *hemB* expression to enhance 5-ALA biosynthesis. However, the overall culture performance was limited by acetogenesis, particularly during extended fed-batch cultivation (data not shown). Note that full abolishment of acetogenesis during aerobic growth of *E. coli* can be highly challenging due to physiological restrictions associated with the carbon overflow metabolism.

4 | DISCUSSION

Being a metabolic intermediate in the pathway for biosynthesis of essential porphyrins, 5-ALA hardly accumulates in *E. coli*. As *hemB* is an essential gene, CRISPRi was applied to repress its expression, such that 5-ALA could accumulate as a result of reduced conversion, with DMH-L1 and DMH-L4 demonstrating high levels of *hemB* repression. Our results further suggest that 5-ALA acts as a committed precursor for porphyrin biosynthesis. Given improved 5-ALA production, *hemB* repression also slightly impaired cell growth, presumably as a consequence of lower biosynthesis of essential porphyrins. However, as the overall culture performance was not seriously affected, the feasibility of this genetic strategy was demonstrated.

Although the effects of oxygen supply on 5-ALA biosynthesis were investigated in several organisms (Nishikawa et al., 1999; Yu et al., 2015), little effort on this front was made for *E. coli*. With the implemented Shemin pathway, 5-ALA biosynthesis in *E. coli* can critically depend on the availability of the key precursor succinyl-CoA, whose formation is rather oxygen-sensitive. Using the control strain DMH, the effects of oxygenic conditions on 5-ALA biosynthesis were systematically investigated for cell cultivation under microaerobic (AL-I), semiaerobic (AL-II), and aerobic (AL-III) conditions. Our results show that biosynthesis of 5-ALA and porphyrins was favored by microaerobic conditions, though the low oxygenic level triggered high-level acetogenesis and the associated growth deficiency. Note that similar observations with regard to impaired cell growth and improved 5-ALA biosynthesis were reported previously during the dissolved oxygen shock period in fed-batch cultivation of recombinant *E. coli* (Yang et al., 2013). Nevertheless, our results suggest that, in DMH, most of 5-ALA/porphyrins were derived via the reductive TCA branch, a phenomenon similar to the previous investigation on overexpression of malic enzymes and their positive effects on 5-ALA biosynthesis in *E. coli* grown anaerobically (Shin, Kwon, Kwon, Lee, & Kim, 2007). Thus, it is suggested that the oxidative TCA cycle and glyoxylate shunt minimally contributed toward 5-ALA biosynthesis under oxygen-limiting conditions.

Compared to DMH, blocking the oxidative TCA cycle in DMHΔ*sdhA* could potentially channel more dissimilated carbon flux toward succinyl-CoA as a result of restricted conversion of succinyl-CoA-to-succinate under AL-I and, therefore, improve biosynthesis of 5-ALA and porphyrins with much-reduced acetogenesis. With more

dissimilated carbon flux channeling into the Shemin pathway, porphyrin biosynthesis was reduced by repressing *hemB* expression to enhance 5-ALA accumulation in DMH-L4Δ*sdhA* under AL-I, achieving 5.95 g L^{-1} 5-ALA and with 36.9% yield while minimizing porphyrin biosynthesis. Note that inactivating the oxidative TCA cycle and/or repressing *hemB* expression resulted in uncommon accumulation of formate with reduced acetogenesis, compared to the control strain DMH. Such observation suggests that, under these biochemical and microaerobic conditions, pyruvate formate lyase (PFL; via which formate is coproduced under anaerobic metabolism) could be more active than pyruvate dehydrogenase (PDH; which is active under aerobic metabolism) for the conversion of pyruvate to acetyl-CoA (Durnin et al., 2009). It was also reported that acetate and formate could induce opposite proteome responses in *E. coli* as most proteins induced by one of these two acids are repressed by the other (Kirkpatrick et al., 2001), further signifying antagonistic nature of these two acids.

While the control strain DMH had a low-level biosynthesis of 5-ALA and porphyrins under aerobic conditions such as AL-III, implying a limited carbon flux contribution from the oxidative TCA cycle (and, therefore, limited succinyl-CoA precursor) into the Shemin pathway, repressing *hemB* expression could also significantly increase 5-ALA accumulation in DMH-L4. Inactivating the oxidative TCA cycle in DMH-L4Δ*sdhA* substantially inhibited cell growth with limited glycerol dissimilation and metabolite production under AL-III, suggesting the critical metabolic roles of the TCA oxidative cycle for biomass formation and biosynthesis under aerobic conditions as per previous observations (Guest, 1981; Steinsiek, Frixel, Stagge, & Bettenbrock, 2011). To resolve the apparent succinyl-CoA limitation under AL-III, we explored channeling of the dissimilated carbon flux via a deregulated glyoxylate shunt by mutating *iclR* in DMH-L4Δ*iclR* and observed significantly enhanced 5-ALA biosynthesis. Nevertheless, with an active TCA oxidative cycle in DMH-L4Δ*iclR*, the carbon flux arising from the deregulated glyoxylate shunt could divert at the succinate node to either the oxidative or reductive TCA direction. Importantly, the flux diversion could be prevented with the dissimilated carbon being effectively directed into the Shemin pathway by further mutating *sdhA* for disruption of the oxidative TCA cycle in DMH-L4Δ*sdhA*Δ*iclR*, achieving 6.93 g L^{-1} 5-ALA with 50.9% yield upon its cultivation under AL-III while minimizing porphyrin biosynthesis. Such carbon flux rerouting effects under AL-III could also be observed by the enhanced biosynthesis of 5-ALA and porphyrins (reflected by notable pigmentation of the culture medium in Figure 7-I) in DMHΔ*sdhA*Δ*iclR* compared to DMH. Additionally, note that the inhibited glycerol utilization and cell growth for DMH-L4Δ*sdhA* could be complemented by the *iclR* mutation, suggesting that both the oxidative TCA cycle and glyoxylate shunt contribute to active TCA operation for sustained cell growth and metabolic biosynthesis under aerobic conditions. As presented in this study, our strategies in engineering the TCA cycle for improved succinyl-CoA production generated higher levels of 5-ALA (via Shemin pathway) compared to previous strategies in which carbon flux was directed toward α-ketoglutarate precursor for 5-ALA biosynthesis via the C5 pathway (Noh, Lim, Park, Seo, & Jung, 2017). While similar studies generated comparable 5-ALA titers (Cui et al., 2019; Yu, Yi, Shih, & Ng, 2019; Zhang et al., 2019), our study showed higher 5-ALA yields particularly when no structurally related carbons were supplemented. Future strain engineering for 5-ALA biosynthesis via the Shemin pathway could include tuning of carbon flux via the glyoxylate shunt by manipulation of *aceA* expression which showed physiological advantages over *iclR* inactivation (Noh et al., 2017). In addition, increasing glycine supply by engineering the glycine-serine biosynthetic pathway could potentially benefit 5-ALA biosynthesis as demonstrated previously (Zou et al., 2017).

ACKNOWLEDGMENTS

We greatly appreciate technical assistance in qRT-PCR from Mark Bruder and Dr. Marc Aucoin. This study was supported by the following Government of Canada grants: Natural Sciences and Engineering Research Council (NSERC) Strategic Partnership grant 430106-12; and Canada Research Chair (CRC) grant 950-211471.

AUTHOR CONTRIBUTIONS

Dragan Miscevic conceived the study, formulated research plan, coordinated research team, carried out experiments, performed result interpretation and data analysis, and drafted the manuscript. Ju-Yi Mao and Teshager Kefale helped to carry out experiments. Daryoush Abedi, Murray Moo-Young, and C. Perry Chou conceived, planned, supervised, and managed the study, as well as helped to draft the manuscript. All authors read and approved the final manuscript.

CONFLICT OF INTERESTS

The authors declare that there are no conflict of interests.

ORCID

C. Perry Chou http://orcid.org/0000-0002-7254-8118

REFERENCES

Arikawa, Y., Kobayashi, M., Kodaira, R., Shimosaka, M., Muratsubaki, H., Enomoto, K., & Okazaki, M. (1999). Isolation of sake yeast strains possessing various levels of succinate- and/or malate-producing abilities by gene disruption or mutation. *Journal of Bioscience and Bioengineering*, *87*, 333–339.

Asakura, T., & Yonetani, T. (1969). Studies on cytochrome *c* peroxidase Xiv. Recombination of apoenzyme with protoheme dialkyl esters and etioheme. *Journal of Biological Chemistry*, *244*, 4573–4579.

Baba, T., Ara, T., Hasegawa, M., Takai, Y., Okumura, Y., Baba, M., … Mori, H. (2006). Construction of *Escherichia coli* K-12 in-frame, single-gene knockout mutants: The Keio collection. *Molecular Systems Biology*, *2*, 1–11.

Cheng, K.-K., Wang, G.-Y., Zeng, J., & Zhang, J.-A. (2013). Improved succinate production by metabolic engineering. *Biomedical Research International*, *2013*, 1–12.

Cherepanov, P. P., & Wackernagel, W. (1995). Gene disruption in *Escherichia coli*: TcR and KmR cassettes with the option of Flp-catalyzed excision of the antibiotic-resistance determinant. *Gene*, *158*, 9–14.

Ciriminna, R., Pina, C. D., Rossi, M., & Pagliaro, M. (2014). Understanding the glycerol market. *European Journal of Lipid Science and Technology*, *116*, 1432–1439.

Cress, B. F., Leitz, Q. D., Kim, D. C., Amore, T. D., Suzuki, J. Y., Linhardt, R. J., & Koffas, M. A. (2017). CRISPRi-mediated metabolic engineering of *E. coli* for O-methylated anthocyanin production. *Microbial Cell Factories*, *16*, 1–14.

Cui, Z., Jiang, Z., Zhang, J., Zheng, H., Jiang, X., Gong, K., … Qi, Q. (2019). Stable and efficient biosynthesis of 5-aminolevulinic acid using plasmid-free *Escherichia coli*. *Journal of Agricultural and Food Chemistry*, *67*, 1478–1483.

Datsenko, K. A., & Wanner, B. L. (2000). One-step inactivation of chromosomal genes in *Escherichia coli* K-12 using PCR products. *Proceedings of the National Academy of Sciences*, *97*, 6640–6645.

Ding, W., Weng, H., Du, G., Chen, J., & Kang, Z. (2017). 5-Aminolevulinic acid production from inexpensive glucose by engineering the C4 pathway in *Escherichia coli*. *Journal of Industrial Microbiology & Biotechnology*, *44*, 1127–1135.

Durnin, G., Clomburg, J., Yeates, Z., Alvarez, P. J. J., Zygourakis, K., Campbell, P., & Gonzalez, R. (2009). Understanding and harnessing the microaerobic metabolism of glycerol in *Escherichia coli*. *Biotechnology and Bioengineering*, *103*, 148–161.

Guest, J. R. (1981). Partial replacement of succinate dehydrogenase function by phage- and plasmid-specified fumarate reductase in *Escherichia coli*. *Journal of General Microbiology*, *122*, 171–179.

Ha, H.-J., Lee, S.-K., Ha, Y.-J., & Park, J.-W. (1994). Selective bromination of ketones. A convenient synthesis of 5-aminolevulinic acid. *Synthetic Communications*, *24*, 2557–2562.

Hotta, Y., Tanaka, T., Takaoka, H., Takeuchi, Y., & Konnai, M. (1997). Promotive effects of 5-aminolevulinic acid on the yield of several crops. *Plant Growth Regulation*, *22*, 109–114.

Inoue, K. (2017). 5-Aminolevulinic acid-mediated photodynamic therapy for bladder cancer. *International Journal of Urology*, *24*, 97–101.

Jobling, M. G., & Holmes, R. K. (1990). Construction of vectors with the p15a replicon, kanamycin resistance, inducible lacZ alpha and pUC18 or pUC19 multiple cloning sites. *Nucleic Acids Research*, *18*, 5315–5316.

Juzeniene, A., Juzenas, P., Iani, V., & Moan, J. (2002). Topical application of 5-aminolevulinic acid and its methylester, hexylester and octylester derivatives: Considerations for dosimetry in mouse skin model. *Photochemistry and Photobiology*, *76*, 329–334.

Kang, D.-K., Kim, S., Chi, W. J., Hong, S. K., Kim, H. K., & Kim, H. U. (2004). Cloning and expression of the *Rhodobacter capsulatus hemA* gene in *E. coli* for the production of 5-aminolevulinic acid. *Journal of Microbiology and Biotechnology*, *14*, 1327–1332.

Kang, Z., Ding, W., Gong, X., Liu, Q., Du, G., & Chen, J. (2017). Recent advances in production of 5-aminolevulinic acid using biological strategies. *World Journal of Microbiology and Biotechnology*, *33*, 200–207.

Kang, Z., Wang, Y., Gu, P., Wang, Q., & Qi, Q. (2011). Engineering *Escherichia coli* for efficient production of 5-aminolevulinic acid from glucose. *Metabolic Engineering*, *13*, 492–498.

Kawakami, H., Ebata, T., & Matsushita, H. (1991). A new synthesis of 5-aminolevulinic acid. *Agricultural and Biological Chemistry*, *55*, 1687–1688.

Kim, S. K., Han, G. H., Seong, W., Kim, H., Kim, S.-W., Lee, D.-H., & Lee, S.-G. (2016). CRISPR interference-guided balancing of a biosynthetic mevalonate pathway increases terpenoid production. *Metabolic Engineering*, *38*, 228–240.

Kim, S. K., Seong, W., Han, G. H., Lee, D.-H., & Lee, S.-G. (2017). CRISPR interference-guided multiplex repression of endogenous competing pathway genes for redirecting metabolic flux in *Escherichia coli*. *Microbial Cell Factories*, *16*, 188–203.

Kirkpatrick, C., Maurer, L. M., Oyelakin, N. E., Yoncheva, Y. N., Maurer, R., & Slonczewski, J. L. (2001). Acetate and formate stress: Opposite responses in the proteome of *Escherichia coli*. *Journal of Bacteriology*, *183*, 6466–6477.

Labun, K., Montague, T. G., Gagnon, J. A., Thyme, S. B., & Valen, E. (2016). CHOPCHOP v2: A web tool for the next generation of CRISPR genome engineering. *Nucleic Acids Research*, *44*, 272–276.

Li, J. M., Brathwaite, O., Cosloy, S. D., & Russell, C. S. (1989). 5-Aminolevulinic acid synthesis in *Escherichia coli*. *Journal of Bacteriology*, *171*, 2547–2552.

Li, S., Jendresen, C. B., Grünberger, A., Ronda, C., Jensen, S. I., Noack, S., & Nielsen, A. T. (2016). Enhanced protein and biochemical production using CRISPRi-based growth switches. *Metabolic Engineering*, *38*, 274–284.

Li, Y., Li, Z., & Wang, L. (2016). Applications of 5-aminolevulinic acid on the physiological and biochemical characteristics of strawberry fruit during postharvest cold storage. *Ciência Rural*, *46*, 2103–2109.

Li, Y. T., Hsieh, Y. L., Henion, J. D., & Ganem, B. (1993). Studies on heme binding in myoglobin, hemoglobin, and cytochrome c by ion spray mass spectrometry. *Journal of the American Society for Mass Spectrometry*, *4*, 631–637.

MacDonald, S. (1974). Methyl 5-bromolevulinate. *Canadian Journal of Chemistry*, *52*, 3257–3258.

Mauzerall, D., & Granick, S. (1956). The occurrence and determination of δ-aminolevulinic acid and porphobilinogen in urine. *Journal of Biological Chemistry*, *219*, 435–446.

Meng, Q., Zhang, Y., Ju, X., Ma, C., Ma, H., Chen, J., … Chen, T. (2016). Production of 5-aminolevulinic acid by cell free multi-enzyme catalysis. *Journal of Biotechnology*, *226*, 8–13.

Miller, J. H. (1992). *A short course in bacterial genetics: A laboratory manual and handbook for* Escherichia coli *and related bacteria* New York: Cold Spring Harbor Laboratory Press.

Murarka, A., Dharmadi, Y., Yazdani, S. S., & Gonzalez, R. (2008). Fermentative utilization of glycerol by *Escherichia coli* and its implications for the production of fuels and chemicals. *Applied and Environmental Microbiology*, *74*, 1124–1135.

Neidhardt, F. C., Bloch, P. L., & Smith, D. F. (1974). Culture medium for enterobacteria. *Journal of Bacteriology*, *119*, 736–747.

Nishikawa, S., Watanabe, K., Tanaka, T., Miyachi, N., Hotta, Y., & Murooka, Y. (1999). *Rhodobacter sphaeroides* mutants which accumulate 5-aminolevulinic acid under aerobic and dark conditions. *Journal of Bioscience and Bioengineering*, *87*, 798–804.

Noh, M. H., Lim, H. G., Park, S., Seo, S. W., & Jung, G. Y. (2017). Precise flux redistribution to glyoxylate cycle for 5-aminolevulinic acid production in *Escherichia coli*. *Metabolic Engineering*, *43*, 1–8.

O'Brian, M. R. (2009). Heme biosynthesis. In M. Schaechter (Ed.), *Encyclopedia of microbiology* (3rd ed., pp. 194–209). Oxford: Academic Press.

Padmanaban, G., Venkateswar, V., & Rangarajan, P. N. (1989). Haem as a multifunctional regulator. *Trends in Biochemical Sciences*, *14*, 492–496.

Pengpumkiat, S., Koesdjojo, M., Rowley, E. R., Mockler, T. C., & Remcho, V. T. (2016). Rapid synthesis of a long double-stranded oligonucleotide from a single-stranded nucleotide using magnetic beads and an oligo library. *PLOS One*, *11*, 1–10.

Petříčková, K., Chroňáková, A., Zelenka, T., Chrudimský, T., Pospíšil, S., Petříček, M., & Krištůfek, V. (2015). Evolution of cyclizing 5-aminolevulinate synthases in the biosynthesis of actinomycete secondary metabolites: Outcomes for genetic screening techniques. *Frontiers in Microbiology*, *6*, 1–15.

Ponka, P. (1999). Cell biology of heme. *The American Journal of the Medical Sciences*, *318*, 241–256.

Qi, L. S., Larson, M. H., Gilbert, L. A., Doudna, J. A., Weissman, J. S., Arkin, A. P., & Lim, W. A. (2013). Repurposing CRISPR as an RNA-guided platform for sequence-specific control of gene expression. *Cell*, *152*, 1173–1183.

Sasaki, K., Watanabe, K., Tanaka, T., Hotta, Y., & Nagai, S. (1995). 5-Aminolevulinic acid production by *Chlorella* sp. during heterotrophic cultivation in the dark. *World Journal of Microbiology and Biotechnology*, *11*, 361–362.

Sasaki, K., Watanabe, M., Tanaka, T., & Tanaka, T. (2002). Biosynthesis, biotechnological production and applications of 5-aminolevulinic acid. *Applied Microbiology and Biotechnology*, *58*, 23–29.

Schlicke, H., Richter, A., Rothbart, M., Brzezowski, P., Hedtke, B., & Grimm, B. (2015). Function of tetrapyrroles, regulation of tetrapyrrole metabolism and methods for analyses of tetrapyrroles. *Procedia Chemistry*, *14*, 171–175.

Shin, J., Kwon, Y. D., Kwon, O., Lee, H. S., & Kim, P. (2007). 5-Aminolevulinic acid biosynthesis in *Escherichia coli* coexpressing NADP-dependent malic enzyme and 5-aminolevulinate synthase. *Journal of Microbiology and Biotechnology*, *17*, 1579–1584.

Skorokhodova, A. Y., Morzhakova, A. A., Gulevich, A. Y., & Debabov, V. G. (2015). Manipulating pyruvate to acetyl-CoA conversion in *Escherichia coli* for anaerobic succinate biosynthesis from glucose with the yield close to the stoichiometric maximum. *Journal of Biotechnology*, *214*, 33–42.

Srirangan, K., Liu, X., Westbrook, A., Akawi, L., Pyne, M. E., Moo-Young, M., & Chou, C. P. (2014). Biochemical, genetic, and metabolic engineering strategies to enhance coproduction of 1-propanol and ethanol in engineered *Escherichia coli*. *Applied Microbiology and Biotechnology*, *98*, 9499–9515.

Steinsiek, S., Frixel, S., Stagge, S., & Bettenbrock, K. (2011). Characterization of *E. coli* MG1655 and *frdA* and *sdhC* mutants at various aerobiosis levels. *Journal of Biotechnology*, *154*, 35–45.

Su, T., Guo, Q., Zheng, Y., Liang, Q., Wang, Q., & Qi, Q. (2019). Fine-tuning of *hemB* using CRISPRi for increasing 5-aminolevulinic acid production in *Escherichia coli*. *Frontiers in Microbiology*, *10*, 1–11.

Takeya, H., Ueki, H., Miyanari, S., Shimizu, T., & Kojima, M. (1996). A new synthesis of 5-aminolevulinic acid via dye-sensitized oxygenation of N-furfurylphthalimide. *Journal of Photochemistry and Photobiology, A: Chemistry*, *94*, 167–171.

Thakker, C., Martinez, I., San, K. Y., & Bennett, G. N. (2012). Succinate production in *Escherichia coli*. *Biotechnology Journal*, *7*, 213–224.

Tran, N. T., Pham, D. N., & Kim, C.-J. (2019). Production of 5-aminolevulinic acid by recombinant *Streptomyces coelicolor* expressing *hemA* from *Rhodobacter sphaeroides*. *Biotechnology and Bioprocess Engineering*, *24*, 488–499.

Wang, L., Elliott, M., & Elliott, T. (1999). Conditional stability of the HemA protein (glutamyl-tRNA reductase) regulates heme biosynthesis in *Salmonella typhimurium*. *Journal of Bacteriology*, *181*, 1211–1219.

Woodard, S. I., & Dailey, H. A. (1995). Regulation of heme biosynthesis in *Escherichia coli*. *Archives of Biochemistry and Biophysics*, *316*, 110–115.

Woolston, B. M., Emerson, D. F., Currie, D. H., & Stephanopoulos, G. (2018). Rediverting carbon flux in *Clostridium ljungdahlii* using CRISPR interference (CRISPRi). *Metabolic Engineering*, *48*, 243–253.

Wu, J., Yu, O., Du, G., Zhou, J., & Chen, J. (2014). Fine-tuning of the fatty acid pathway by synthetic antisense RNA for enhanced (2*S*)-naringenin production from L-tyrosine in *Escherichia coli*. *Applied and Environmental Microbiology*, *80*, 7283–7292.

Yang, J., Zhu, L., Fu, W., Lin, Y., Lin, J., & Cen, P. (2013). Improved 5-aminolevulinic acid production with recombinant *Escherichia coli* by a short-term dissolved oxygen shock in fed-batch fermentation. *Chinese Journal of Chemical Engineering*, *21*, 1291–1295.

Yazdani, S. S., & Gonzalez, R. (2007). Anaerobic fermentation of glycerol: A path to economic viability for the biofuels industry. *Current Opinion in Biotechnology*, *18*, 213–219.

Yu, T.-H., Yi, Y.-C., Shih, I.-T., & Ng, I.-S. (2019). Enhanced 5-aminolevulinic acid production by co-expression of codon-optimized *hemA* gene with chaperone in genetic engineered *Escherichia coli*. *Applied Biochemistry and Biotechnology*, *191*, 299–312.

Yu, X., Jin, H., Liu, W., Wang, Q., & Qi, Q. (2015). Engineering *Corynebacterium glutamicum* to produce 5-aminolevulinic acid from glucose. *Microbial Cell Factories*, *14*, 1–10.

Zhang, B., & Ye, B.-C. (2018). Pathway engineering in *Corynebacterium glutamicum* S9114 for 5-aminolevulinic acid production. *3 Biotech*, *8*, 247–257.

Zhang, J., Kang, Z., Chen, J., & Du, G. (2015). Optimization of the heme biosynthesis pathway for the production of 5-aminolevulinic acid in *Escherichia coli*. *Scientific Reports*, *5*, 1–7.

Zhang, J., Weng, H., Zhou, Z., Du, G., & Kang, Z. (2019). Engineering of multiple modular pathways for high-yield production of 5-aminolevulinic acid in *Escherichia coli*. *Bioresource Technology*, *274*, 353–360.

Zou, Y., Chen, T., Feng, L., Zhang, S., Xing, D., & Wang, Z. (2017). Enhancement of 5-aminolevulinic acid production by metabolic engineering of the glycine biosynthesis pathway in *Corynebacterium glutamicum*. *Biotechnology Letters*, *39*, 1369–1374.

SUPPORTING INFORMATION

Additional Supporting Information may be found online in the supporting information tab for this article.

How to cite this article: Miscevic D, Mao J, Kefale T, Abedi D, Moo-Young M, Perry Chou C. Strain engineering for high-level 5-aminolevulinic acid production in *Escherichia coli*. *Biotechnology and Bioengineering*. 2020;1–13.
https://doi.org/10.1002/bit.27547